Atypical development of white matter microstructure in adolescents with autism spectrum disorders

Yawei Cheng [a,b], Kun-Hsien Chou [c], I-Yun Chen [a], Yang-Teng Fan [a], Jean Decety [d], Ching-Po Lin [a,*]

[a] *Institute of Neuroscience, National Yang-Ming University, 155 Li-Nong St., Sec. 2, Peitou, Taipei, Taiwan*
[b] *Department of Physical Medicine and Rehabilitation, National Yang-Ming University Hospital, Yilan, Taiwan*
[c] *Institute of Bioengineering, National Yang-Ming University, Taipei, Taiwan*
[d] *Departments of Psychology and Psychiatry, Center for Cognitive and Social Neuroscience, The University of Chicago, Chicago, IL, USA*

ARTICLE INFO

ABSTRACT

Diffusion tensor imaging (DTI) studies in adolescents with autism spectrum disorders (ASD) indicate aberrant neurodevelopment of frontal white matter (WM), potentially underlying abnormal social cognition and communication in ASD. Here, we further use tract-based spatial statistics (TBSS) to examine the developmental change of WM skeleton (i.e., the most compact whole-brain WM) during adolescence in ASD. This whole-brain DTI used TBSS measures fractional anisotropy (FA) and longitudinal and radial diffusivities in fifty adolescents, 25 ASD and 25 controls. Results show that adolescents with ASD versus controls had significantly reduced FA in the right posterior limb of internal capsule (increased radial diffusivity distally and reduced longitudinal diffusivity centrally). Adolescents with ASD versus controls (covarying for age and IQ) had significantly greater FA in the frontal lobe (reduced radial diffusivity), right cingulate gyrus (reduced radial diffusivity), bilateral insula (reduced radial diffusivity and increased longitudinal diffusivity), right superior temporal gyrus (reduced radial diffusivity), and bilateral middle cerebellar peduncle (reduced radial diffusivity). Notably, a significant interaction with age by group was found in the right paracentral lobule and bilateral superior frontal gyrus as indicated by an age-related FA gain in the controls whilst an age-related FA loss in the ASD. To our knowledge, this is the first study to use TBSS to examine WM in individuals with ASD. Our findings indicate that the frontal lobe exhibits abnormal WM microstructure as well as an aberrant neurodevelopment during adolescence in ASD, which support the frontal disconnectivity theory of autism.

© 2010 Elsevier Inc. All rights reserved.

Introduction

Autism spectrum disorders (ASD) is a relative common brain developmental disorder that occurs in one in 150 children (Van Naarden Braun et al., 2007). It is characterized by early onset of impaired social reciprocity and communication difficulties, along with restricted interest and stereotyped behavior (WHO, 1994). Several lines of evidence suggest that cascade failure of neurodevelopment is most likely the core deficit of ASD (Amaral et al., 2008; Baron-Cohen and Belmonte, 2005; Courchesne and Pierce, 2005a; Courchesne et al., 2007; Geschwind and Levitt, 2007). Using tract-based spatial statistics (TBSS) on the quantitative indices from diffusion tensor imaging (DTI), the present study aimed to examine the developmental change of white matter (WM) skeleton during adolescence in ASD.

Currently, several lines of evidence suggest that the brain of ASD individuals, as indexed by head circumference and brain volume, undergoes a period of precocious growth during early postnatal life

followed by a deceleration in age-related growth, as compared to typically developing children (Courchesne et al., 2003; Dawson et al., 2007; Dementieva et al., 2005; Sparks et al., 2002). Disproportional increases in WM were postulated to account for this abnormal brain enlargement, as indicated by studies of young children (Courchesne et al., 2003; Dementieva et al., 2005; Herbert et al., 2003; Herbert et al., 2004). In addition, abnormal structures of the gray matter may be related to malformations of the WM, which is especially intriguing in ASD considering the fact that the cognitive deficit is most likely to arise from impaired integrative processing through intrahemispheric and interhemispheric transfer of information (Just et al., 2004; Minshew et al., 1997). Thus, whether aberrant WM development persists into later childhood and adolescence is a crucial issue to probe (Hazlett et al., 2006; Lotspeich et al., 2004; Palmen et al., 2005).

With the advent of DTI, a technique based on the measurement of water molecular diffusion, the architecture of human WM tracts can be more thoroughly scrutinized *in vivo* (Engelbrecht et al., 2002; Mukherjee and McKinstry, 2006; Mukherjee et al., 2002; Neil et al., 2002; Neil et al., 1998). In comparison to other MRI measures (e.g., T1- and T2-weighted images), DTI is a much more sensitive measure of WM maturation (Baratti et al., 1999; Huppi et al., 1998; Neil et al.,

---

* Corresponding author. Fax: +886 2 28262285.
 E-mail address: cplin@ym.edu.tw (C.-P. Lin).

1998). Fractional anisotropy (FA) is a quantitative parameter derived from DTI which measures the direction-dependent diffusivity of water molecules, and is an indicator of the diameter and density of fibers, myelination, and macrostructural features (such as fiber tract coherence) of WM fibers (Beaulieu, 2002).

To date, studies that have used DTI measures in ASD are limited (Alexander et al., 2007; Barnea-Goraly et al., 2004; Ben Bashat et al., 2007; Catani et al., 2008; Conturo et al., 2008; Keller et al., 2007; Lee et al., 2007; Sundaram et al., 2008; Thakkar et al., 2008). The manner through which ASD alters FA values remains controversial. For instance, one study reported that the adolescents, ages 11–18 years, with high functioning autism have reduced FA values in brain regions that are implicated in social cognitive processes, such as theory of mind (ventromedial prefrontal cortex, anterior cingulate cortex, temporoparietal junction, superior temporal sulcus, and amygdala) (Barnea-Goraly et al., 2004). Other studies of adults with ASD reported lower FA values in the corpus callosum (Alexander et al., 2007), the genu and splenium of corpus callosum, and the internal capsule (Keller et al., 2007), the superior temporal gyrus (Lee et al., 2007), the cerebellar feedback projections (Catani et al., 2008), and the anterior cingulate gyrus (Thakkar et al., 2008). In contrast, young children with autism had increased FA values in the frontal lobe or no change at all (Ben Bashat et al., 2007). Another study found that an interaction of age by group in the posterior limb of the right internal capsule as shown by an age-related increase in FA values in the ASD participants and an age-related decrease in the controls (Keller et al., 2007). However, superior temporal gyrus displayed minimal change in ASD but an increase in the controls (Lee et al., 2007). Similarly, children with ASD appeared to have an imbalance of FA in the frontal lobe as indicated by lower FA for short range fibers and higher FA for long range association fibers (Sundaram et al., 2008). Thus, we speculated that age is an important factor in determining the brain manifestations observed in ASD.

Furthermore, some issues with DTI analysis should be acknowledged. First, the interpretation of FA changes, particularly increases in FA values in individuals with pathological conditions (e.g., subjects with ASD) vs. controls, needs to be determined. The degree of diffusion anisotropy conventionally described in terms of the FA has been referred to as a measure of the microstructural integrity of WM tissue. Importantly, FA might only provide an indirect marker for the microstructural properties of WM (Tuch et al., 2005). Greater FA may reflect greater myelination of WM fibers, increased number of myelinated fibers, smaller axonal diameter, or reduced neural branches within MRI voxel (Beaulieu, 2002; Hoeft et al., 2007). Alternatively, FA changes may result from excessive partial volume averaging from differently oriented fibers (Beaulieu, 2002; Le Bihan, 1995; Schwartz and Hackney, 2003). Reduced FA has been associated with local edema, cerebrospinal fluid (Mukherjee and McKinstry, 2006; Mukherjee et al., 2002), compromised myelin structure, changes in axonal morphologic structure, and altered interaxonal spacing of fiber bundles (Arfanakis et al., 2002; Beaulieu, 2002; Concha et al., 2005; Thomalla et al., 2004). Therefore, eigenvalues representing measures of longitudinal and radial diffusivities have been derived and validated (Hasan and Narayana, 2006; Song et al., 2002) as more specific measures of diffusivity in the longitudinal diffusion direction and transverse direction, respectively. These measures can help interpret FA changes in WM tracts in pathologic groups by providing information regarding likely alternations in the proportions of longitudinal vs. radial diffusivity. Reduced longitudinal diffusivity may suggest the decline of axonal integrity, and decreased radial diffusivity may be a non-invasive surrogate marker of demyelination (Budde et al., 2008; Song et al., 2003).

A second issue is that DTI analysis is compromised by the use of standard registration algorithms, such that there was not yet a satisfactory convention for the alignment of FA images from multiple subjects in voxel-wise analyses (Smith et al., 2006). A recent advance is to develop TBSS, an automated observer-independent method of aligning FA images from multiple subjects to allow group-wise comparisons of DTI data (Smith et al., 2006; Smith et al., 2007). TBSS focuses on the WM skeleton (i.e., the most compact whole-brain WM). This technique has been used to study preterm infants and adolescent development (Anjari et al., 2007; Giorgio et al., 2008), patients with schizophrenia (Douaud et al., 2007; Karlsgodt et al., 2008), fetal alcohol syndrome (Li et al., 2009), epilepsy (Schoene-Bake et al., 2009), attention deficit hyperactivity disorder (Silk et al., 2008), multiple sclerosis (Bodini et al., 2009; Cader et al., 2007; Dineen et al., 2009; Roosendaal et al., 2009), bipolar disorder (Barnea-Goraly et al., 2009; Versace et al., 2008), amyotrophic lateral sclerosis (Sage et al., 2009), and Alzheimer's disease (Stricker et al., 2009), marijuana users (Arnone et al., 2008), and young adults exposed to parental verbal abuse (Choi et al., 2009), but not, to our knowledge, individuals with ASD.

During adolescence, the structural maturation of fiber tracts in the human brain, including increases in axon myelination and FA, plays a role in cognitive development (Ashtari et al., 2007; Barnea-Goraly et al., 2005; Paus et al., 1999; Schmithorst et al., 2005). Thus, we hypothesized that individuals with ASD might fail to undergo complete maturation of WM tracts, particularly in the frontal lobe, during adolescence. The goal of the present study was to utilize the TBSS method of DTI analysis to investigate differences in FA and longitudinal and radial diffusivities over age in adolescents with ASD and matched controls.

Methods

Participants

All participants were right-handed ethnic Chinese males with IQ>80 as estimated by Wechsler Intelligence Scale for Children (Wechsler, 1991). Adolescents with a co-morbid psychiatric or medical condition (e.g., epilepsy), history of head injury, or genetic disorder associated with autism (e.g., fragile×syndrome) were excluded. The ASD group had twenty-five non-medicated adolescents with ASD aged 10–18 years, recruited from a community autism program. The diagnosis of ASD was confirmed using the DSM-IV diagnostic criteria. Twenty-five typically developing control adolescents aged 11–18 years were recruited from local schools and screened for major psychiatric illness using a structured parental interview. Every adolescent's parents gave informed consent for the protocol approved by local Ethics Committee (Taipei Veterans General Hospital, TPE-VGH), and each adolescent gave his/her assent. This study was conducted in accordance with the Declaration of Helsinki.

Data acquisition

All MR scans were performed on a 1.5 T MR system (Excite II; GE Medical Systems, Milwaukee, Wis., USA) equipped with an 8-channel head coil in TPE-VGH. A three-plane localizer scan was collected to orient subsequent imaging slices parallel to the anterior commissure–posterior commissure line. To diminish motion artifact generated during the scanning, the participant's head was immobilized with cushions inside the coil. High resolution T1-weighted (T1W) anatomical images covering the entire brain were acquired using an axial three-dimensional fluid-attenuated inversion-recovery fast spoiled gradient recalled echo (FLAIR-FSPGR) sequence with parameters: TR = 8.548 ms, TE = 1.836 ms, TI = 400 ms, flip angle = 15°, field of view = 26 cm^2, matrix size = 256×256, number of slice = 124 and slice thickness = 1.5 mm. Diffusion-weighted images were acquired using a single shot spin-echo echo planar imaging (EPI) sequence with TR/TE = 17000/68.9 ms, NEX = 6, field of view = 26 cm^2, matrix size = 128×128, yielding the in-plane resolution of 2 mm. The slice

thickness was 2.2 mm with 70 continuous sections providing total brain coverage. The diffusion images gradient encoding scheme entailed thirteen non-collinear directions with b value of 900 s/mm^2 and a non-diffusion weighted image according to the minimal energy arrangement of electron distribution. The total scanning time to collect the above images was approximately 32 min for each subject. An expert radiologist screened all the Magnetization Prepared Rapid Gradient Echo (MPRAGE) images for visible WM and other pathologic findings as part of our institutional review board-approved protocol.

Data analysis

All data were transferred off-line to a linux-based workstation and processed with FSL 4.1 (Functional Magnetic Resonance Imaging of the Brain Software Library; http://www.fmrib.ox.au.uk/fsl) and in-house software. First, the DICOM files of each DTI acquisition were converted into a single multivolume NIFTI file (Neuroimaging Informatics Technology Initiative file). The diffusion-weighted images were registered to the non-diffusion weighted image by affine transformations to minimize distortions due to eddy currents and to reduce simple head motion using eddy current correction. In order to remove non-brain tissue components and background noise, images were extracted using Brain Extraction Tool (BET), also compiled in FSL 4.1 (Smith, 2002). After preprocessing, a diffusion tensor model was fitted at each voxel using an in-house program to provide a voxel-wise calculation of FA. FA can be expressed in terms of three eigenvalues: $\lambda 1$ represents the magnitude of diffusion along the principal longitudinal diffusion direction. The arithmetical mean of the other two eigenvalues, $\lambda 2$ and $\lambda 3$ $[(\lambda 2 + \lambda 3)/2]$ represents the magnitude of diffusion in the two orthogonal directions perpendicular to the principal diffusion direction.

Whole brain voxel-wise statistic analysis of the FA data was carried out using Tract-Based Spatial Statistics (TBSS) (Smith et al., 2006; Smith et al., 2004), which is implemented in FSL (Oxford, UK). The TBSS method minimizes the potential misalignment problems of other voxel-based whole-brain analysis methods by determining a white-matter "skeleton" restricted only to the center of major white-matter tracts, and mapping FA values from each individual directly onto this standard skeleton for group comparison.

All subject's FA data were aligned into a common space using the nonlinear registration tool FNIRT (www.fmrib.ox.ac.uk/analysis/techrep), which uses a b-spline representation of the registration warp field (Rueckert et al., 1999). The cross-subjects mean FA image was calculated and used to generate a mean FA skeleton representing the centers of all tracts common to the whole study group. The threshold of the mean FA skeleton was set at 0.2 to successfully exclude voxels, which consisted of gray matter or CSF in the majority of subjects. The averaging procedure constrains the skeleton to exclude the tracts at the outermost edges of the cortex, where greater between-subjects variability in tract location causes poor groupwise registration, due to constraints of the nonlinear alignment algorithm. In other words, this method excludes from further analysis those parts of the brain where we do not believe that good tract correspondence across subjects can be achieved (Smith et al., 2006; Smith et al., 2004). Previous studies have also adopted the same threshold for the FA skeleton (Dineen et al., 2009; Giorgio et al., 2008; Versace et al., 2008). Each individual subject's aligned FA data were projected onto this masked skeleton by filling the skeleton with FA values from the nearest relevant tract center. The skeletonized FA data were fed into the following voxel-wise cross-subjects statistics which were based on non-parametric permutation test (Randomise; part of FSL tool; http://www.fmrib.ox.ac.uk/fsl/randomise/index.html).

In order to identify FA difference between two groups, nonparametric two-sample independent t-tests were used to compare groups based on a permutation method because of the substantial non-Gaussian distribution of the FA data (Jones et al., 2005; Karlsgodt et al.,

2008; Smith et al., 2006). Age and IQ were entered into this analysis as confounding factors to ensure that any observed difference of group on FA was independent of age-and IQ-related changes. The procedure of statistical inference, which we used here, was the same used in previous TBSS studies (Anjari et al., 2007; Smith et al., in press; Versace et al., 2008). Inference was carried out using a threshold (t value>3.0; $P<0.001$ uncorrected; the number of permutations: 5000 without variance smoothing; extent threshold>10 contiguous voxels). We further controlled for multiple voxel-level comparisons within each significant cluster using the Small Volume Correction (SVC) ($P<0.05$) in FSL [False Discovery Rate (FDR); http://www.fmrib.ox.ac.uk/fsl/randomise/fdr.html], employing an anatomically defined regional mask in the relevant WM tract containing approximately 100 times the number of voxels of each cluster. Only the clusters surviving the voxel-level SVC-FDR $P<0.05$ are reported. We determined the most probable anatomic localization of each cluster by means of the FSL atlas tool (http://www.fmrib.ox.ac.uk/fsl /fslview/atlas-descriptions.html/), which incorporates several anatomic templates, including the Talairach atlas, MNI structural atlas, Julich histological atlas, Oxford thalamic connectivity atlas, Harvard-Oxford cortical and subcortical structural atlases, and the Johns Hopkins University DTI-based WM atlases. All reported brain images were acquired using the "tbss_fill" script from the FSL package.

Whole-Brain voxelwise analysis of Longitudinal and Radial diffusivities

Longitudinal (principle longitudinal direction, $\lambda 1$) and radial (transverse diffusion component, $[(\lambda 2 + \lambda 3)/2]$ diffusivity values were computed for all clusters showing a significant FA change (increase or decrease) between subjects with ASD and controls surviving the statistical constraints described above.

Interaction analysis of age by groups

To elucidate different developmental pattern between the two groups, we performed a voxel-by-voxel interaction analysis of age by group (ASD vs. controls) using a step-up hierarchical multiple regression strategy (Keller et al., 2007; Nunnemann et al., 2009). We first examined the main effects of group on FA, with age and full-scale IQ entered as additional covariates, and then tested for areas showing linear interactions between group and age by including the product of group and age in the model.

The statistic criteria of this interaction analysis were the same as described above for the group comparison, using SVC ($P<0.05$) with an anatomically defined regional mask in the relevant WM tract, containing approximately 100 times the number of voxels of each cluster, calculated using an FSL statistical tool (FDR). For the clusters showing significant interaction, the mean FA value (i.e., the mean of all voxel FA values within the cluster) was analyzed separately for ASD and controls with standard software (SPSS, version 14.0.1).

Results

Demographics

The characteristics of the participants were listed in Table 1. The ASD group consisted of 25 participants with the diagnosis at the time of DTI: 11 autism, 12 Asperger's disorder, and 2 pervasive developmental disorders not otherwise specified. The subjects with ASD and the controls were group-matched on age, full-scale IQ, and handedness.

Direct group comparisons

Controlling for age and IQ as covariates, the exploratory groupwise comparison of the ASD group and the controls (SVC-FDR-corrected $P<0.05$, Z score>3.15) showed that individuals with ASD exhibited greater FA in several clusters including the right superior longitudinal

Table 1
Demographic and clinical variables.

Variable and group	Mean (SD)	Statistic	2-Tailed P value
Age at imaging (years)		$t(48)=0.35$	0.73
ASD ($n=25$)	13.71 (2.54)		
Control ($n=25$)	13.51 (2.20)		
Full scale intelligence quotient		$t(48)=-1.61$	0.12
ASD	101.60 (18.91)		
Control	109.04 (9.45)		

Abbreviation: ASD, autism spectrum disorder.

fasciculus of middle frontal gyrus, right cingulate gyrus, right superior corona radiata of frontal lobe, right postcentral gyrus, bilateral insula, right anterior thalamus, right putamen, right superior temporal gyrus, right inferior occipital gyrus, and bilateral middle cerebellar peduncle (Table 2 and Fig. 1). Notably, the cluster in the right middle cerebellar peduncle had greater FA associated with greater longitudinal diffusivity ($P\leq0.001$) and a trend-level reduction in radial diffusivity ($P<0.003$) among subjects with ASD vs. controls. The left insula and right superior corona radiata had a trend-level decrease in radial diffusivity ($P\leq0.018$; $P\leq0.005$, respectively) but no change in longitudinal diffusivity ($P=0.350$; $P=0.400$, respectively). In the other clusters, greater FA was associated with significantly reduced radial diffusivity ($P\leq0.001$).

Conversely, there were some regions with lower FA in subjects with ASD vs. controls. The regions included clusters of right angular gyrus, left globus pallidus, and right inferior cerebellar peduncle (Fig. 2 and Table 2). Lower FA in the right angular gyrus was associated with decreased longitudinal diffusivity and increased radial diffusivity among subjects with ASD vs. controls ($P\leq0.001$; and $P\leq0.001$, respectively). However, the left globus pallidus cluster had a reduction in longitudinal diffusivity but no change in radial diffusivity ($P\leq0.001$; $P=0.011$, respectively), and the right

inferior cerebellar peduncle had an increase in radial diffusivity but only a trend change in longitudinal diffusivity ($P\leq0.001$; $P=0.003$, respectively). In addition, among these clusters, the correlations of FA with age in these clusters within each group separately were demonstrated (Supplementary Material).

Interaction of age by groups

Table 3 shows the analysis of the interaction of age by groups (ASD vs. controls). Notably, the interaction effect mainly occurs in the frontal lobe, including bilateral superior frontal gyrus, right paracentral lobule, right cingulate gyrus, corpus callosum, and right inferior occipitofrontal fasciculus, as indicated by age-related gains in WM integrity in the controls and losses in the ASD group. Specifically, the FA value of paracentral lobule (the mean of all voxels in the clusters, peak [x, y, z] = 7, −35, 53) had a significantly positive correlation with age in the controls (Pearson correlation coefficient $r=0.630$, two-sided P value = 0.001) but a trend-leveled negative correlation in the ASD (Pearson correlation coefficient $r=-0.464$, two-sided P value = 0.020). Similarly, in the right and left superior frontal gyrus (peak [x, y, z] = 10, 34, 47; −9, 14, 57), the controls showed an age-related gain of regional WM integrity ($r=0.661$, two-sided P value < 0.001; $r=0.677$, two-sided P value < 0.001) but the ASD group did not change with age significantly ($r=-0.343$, two-sided P value = 0.093; $r=-0.044$ two-sided P value < 0.835) (Fig. 3).

Discussion

Previous DTI studies in individuals with ASD have reported that FA increases at an abnormally accelerated rate during early childhood development (Ben Bashat et al., 2007) while other studies have reported decreases in FA during adolescence and early adulthood (Alexander et al., 2007; Barnea-Goraly et al., 2004; Catani et al., 2008; Conturo et al., 2008; Lee et al., 2007; Sundaram et al., 2008; Thakkar et al., 2008). Here, we demonstrate an FA imbalance between

Table 2
Regions showing greater and reduced fractional anisotropy (FA) in 25 subjects with autism spectrum disorder (ASD) vs. in 25 control subjects.

MNI atlas coordinates			Voxel size	White matter tract	Corresponding cortical area	FA Mean (SD)		t_{max}	Diffusivity Values		Cohen d
x	y	z				ASD	Control		Longitudinal	Radial	
Increased FA in Subjects with ASD vs. Control											
34	−9	41	20	Right superior longitudinal fasciculus	Middle Frontal Gyrus	0.551 (0.051)	0.479 (0.055)	**4.3**	−17.20	**69.84*****	1.39
17	3	36	28	Right superior corona radiata	Cingulate Gyrus	0.528 (0.035)	0.466 (0.043)	**5.4**	−14.92	**56.56*****	1.62
26	−10	32	11	Right superior corona radiata	Frontal Lobe	0.482 (0.055)	0.433 (0.029)	**4.1**	5.17	**47.79*****	1.14
26	−18	28	22	Right superior corona radiata	Frontal Lobe	0.575 (0.040)	0.530 (0.044)	**3.8**	−13.81	**35.62****	1.11
36	−29	29	19	Right superior longitudinal fasciculus	Postcentral Gyrus	0.535 (0.042)	0.488 (0.044)	**4.0**	−31.58	**38.78*****	1.11
34	−32	25	21	Right superior longitudinal fasciculus	Insula	0.402 (0.035)	0.356 (0.024)	**5.3**	−12.51	**39.35*****	1.56
35	−12	25	17	Right superior longitudinal fasciculus	Insula	0.493 (0.048)	0.443 (0.045)	**3.6**	−41.66$^{\psi}$	34.73$^{\psi}$	1.09
38	−41	24	14	Right superior longitudinal fasciculus	Insula	0.512 (0.070)	0.452 (0.039)	**3.7**	−19.08	**59.34*****	1.09
−33	21	−3	17	Left insula	Insula	0.323 (0.042)	0.266 (0.036)	**3.9**	46.98	90.32$^{\psi}$	1.49
9	−6	12	16	Right anterior thalamic radiation	Thalamus	0.433 (0.045)	0.379 (0.057)	**3.9**	15.17	**63.15*****	1.09
26	−18	10	18	Right posterior limb of	Putamen	0.704 (0.032)	0.664 (0.038)	**4.3**	−15.55	**34.50*****	1.17
25	−14	9	14	Right posterior limb of internal capsule	Putamen	0.776 (0.033)	0.733 (0.041)	**3.9**	−6.28	**48.47*****	1.21
52	−29	8	14	Right superior longitudinal fasciculus	Superior Temporal Gyrus	0.501 (0.060)	0.429 (0.052)	**4.0**	−84.21*	**43.99*****	1.31
36	−71	−5	15	Right inferior occipitofrontal fasciculus	Inferior Occipital Gyrus	0.477 (0.050)	0.416 (0.047)	**4.1**	−48.08$^{\psi}$	**47.04*****	1.29
31	−48	−39	42	Right middle cerebellar peduncle	Cerebellar Tonsil	0.686 (0.046)	0.615 (0.064)	**4.7**	**−100.37*****	36.54**	1.30
−17	−45	−39	16	Left middle cerebellar peduncle	Cerebellar Tonsil	0.625 (0.045)	0.554 (0.054)	**5.0**	−73.89*	**43.59*****	1.46
Decreased FA in Subjects with ASD vs. Control											
38	−58	35	32	Right superior longitudinal fasciculus	Angular Gyrus	0.368 (0.098)	0.485 (0.072)	**4.9**	**126.76*****	**−72.85*****	1.38
−19	−15	−2	17	Left posterior limb of internal capsule	Globus Pallidus	0.748 (0.029)	0.785 (0.034)	**4.1**	**78.58*****	−30.92$^{\psi}$	1.18
11	−45	−47	21	Right inferior cerebellar peduncle	Medulla	0.283 (0.073)	0.378 (0.088)	**4.4**	−397.42**	**−388.55*****	1.20

Boldfaced FA indexes stand for clusters with $t\geq3.0$ ($P\leq0.001$ uncorrected) as well as ≥11 voxels. All these regions survived small-volume corrections (false discovery rate, $P\leq0.05$) to control for multiple tests. Boldfaced longitudinal and radial diffusivity indexes indicate significant differences ($P\leq0.001$ uncorrected) in these clusters. Bonferroni corrections (false discovery rate, $P\leq0.05$) were also conducted in the consideration of multiple comparisons. Abbreviations: MNI, Montreal Neurological Institute.
***$P\leq0.001$; **$P\leq0.005$; *$P\leq0.01$; $^{\psi}P\leq0.05$.
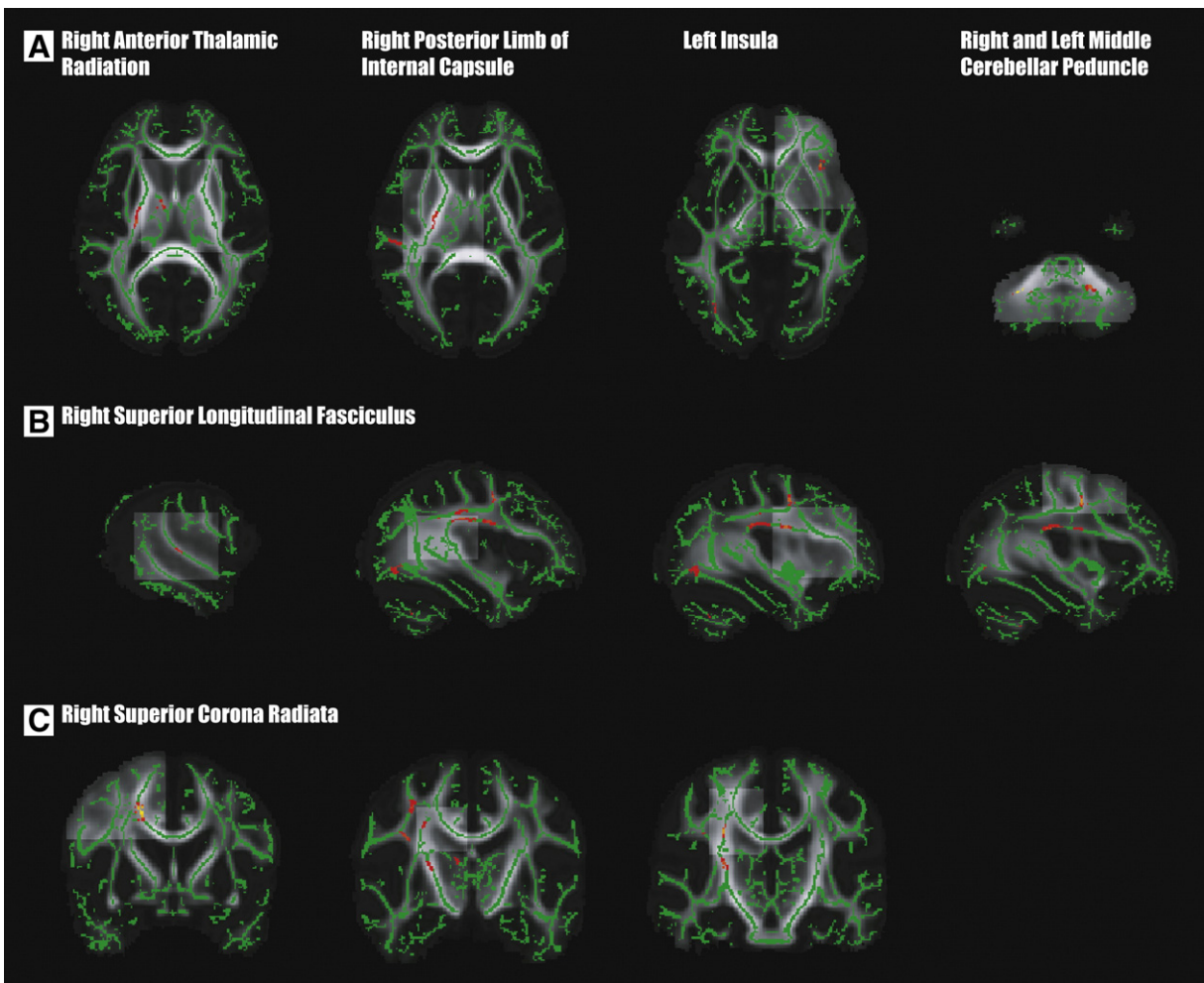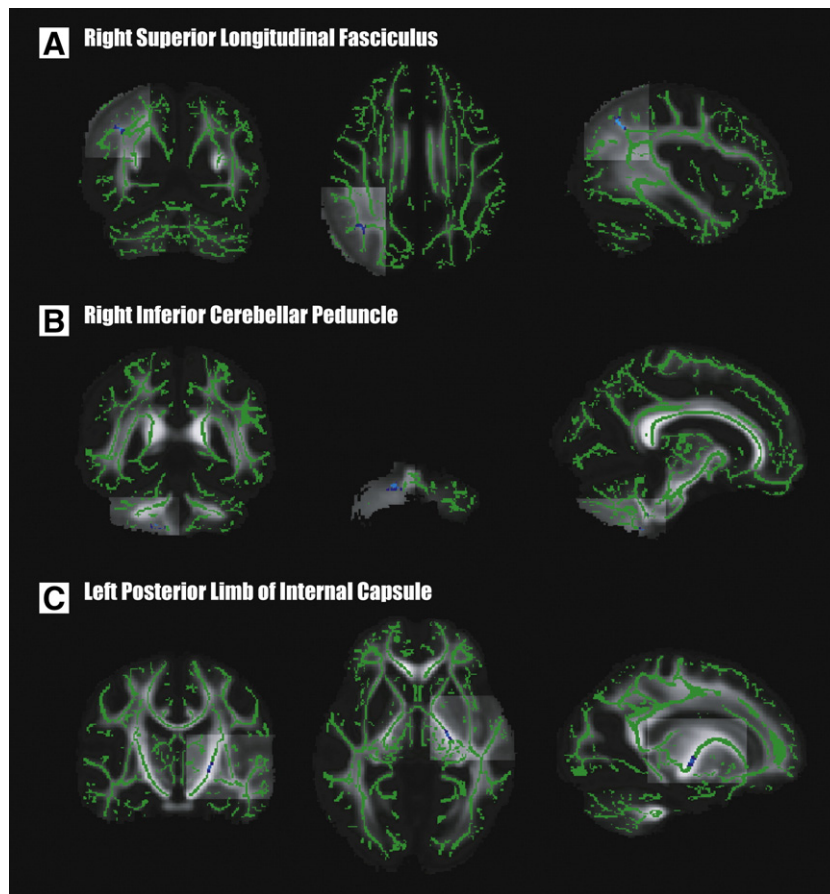
Fig. 1. Regions with significantly higher fractional anisotropy (FA) in subjects with autism spectrum disorder (ASD) vs. controls. The group's mean FA skeleton (green) was overlaid on the mean_whole_group_FA images in the axial, sagittal, and coronal views. The threshold of mean FA skeleton was set at 0.2. The regions with significantly higher FA in subjects with ASD vs. controls were highlighted on the mean FA skeleton in colored voxels (scale ranging from red to yellow). The statistical criterion for between-group differences was set at $P<0.05$ corrected for multiple comparisons across voxels. (A) The central cluster in the right anterior thalamic radiations, posterior limb of internal capsule, left insula, and bilateral middle cerebellar peduncle. (B) The right insula and superior temporal gyrus clusters in the superior longitudinal fasciculus. (C) The cingulate gyrus cluster in the right corona radiata.

control and ASD adolescent groups, indicated by less FA in the right angular gyrus, left globus pallidus, and right inferior cerebellar peduncle, but greater FA in the right superior longitudinal fasciculus of middle frontal gyrus, right cingulate gyrus, right superior corona radiata of frontal lobe, right postcentral gyrus, bilateral insula, right anterior thalamus, right putamen, right superior temporal gyrus, right inferior occipital gyrus, and bilateral middle cerebellar peduncle. Notably, the frontal cortex FA, including clusters of the bilateral superior frontal gyrus, right paracentral lobule, right cingulate gyrus, corpus callosum, and right inferior occipitofrontal fasciculus displayed a significant interaction of age by group as shown by age-related gains in the control compared to no significant age-related change in the ASD group.

The distributed locations of FA imbalances revealed in the direct group comparison (ASD vs. controls) are consistent with previous studies. For instance, some studies reported that FA was reduced in the prefrontal cortex, anterior cingulate, superior temporal gyrus, corpus callosum, and superior cerebellar peduncle (Alexander et al., 2007; Barnea-Goraly et al., 2004; Catani et al., 2008; Keller et al., 2007; Lee et al., 2007; Thakkar et al., 2008). Specifically, FA was reduced for short range fibers within frontal lobe (Sundaram et al., 2008). However, other studies reported increased FA during childhood and adolescence in ASD (Ashtari et al., 2007; Ben Bashat et al., 2007). Here,

we used TBSS and found WM integrity imbalance as indicated by FA increases in the frontal lobe, right cingulate gyrus, right postcentral gyrus, bilateral insula, right anterior thalamus, right superior temporal gyrus, and bilateral middle cerebellar peduncle, and decrease in the right angular gyrus, left globus pallidus, and right inferior cerebellar peduncle. We thus argue that the FA imbalance observed in ASD may result from developmental aberrance of the WM skeletons.

The FA imbalance in ASD may reflect aberrant WM neurodevelopment. A number of studies, through measures including head circumference, neuroimaging, and postmortem investigations, reported that the autistic brain undergoes a period of precocious growth during early postnatal life, followed by a period of decelerated growth (Courchesne et al., 2003; Dawson et al., 2007; Dementieva et al., 2005). Notably, in individuals with ASD, the amygdala displays hyperplasia at early developmental timepoints, but ultimately becomes hypoplastic by late childhood and early adolescence, when brain growth in normal subjects has caught up (Schumann and Amaral, 2006; Schumann et al., 2004). We speculate that a critical period for the interaction of age and group may occur around late childhood to early adolescence, as individuals with ASD appear to have greater FA before the period, but decreased FA thereafter. This supports the hypothesis that subjects with ASD may fail to integrate

Fig. 2. Regions with significantly lower fractional anisotropy (FA) in subjects with autism spectrum disorder (ASD) vs. controls. The group's mean FA skeleton (green) was overlaid on the mean_whole_group_FA images in the axial, sagittal, and coronal views. The threshold of mean FA skeleton was set at 0.2. The regions with significantly lower FA in subjects with ASD vs. controls were highlighted on the mean FA skeleton in colored voxels (scale ranging from dark blue to light blue). The statistical criterion for between-group differences was set at $P<0.05$ corrected for multiple comparisons across voxels. (A) The angular gyrus cluster in the superior longitudinal fasciculus. (B) The inferior cerebellar peduncle. (C) The left posterior limb of internal capsule.

appropriate environmental influences to guild selective and effective synapse elimination during the second wave of exuberant synapto-genesis that occurs in typically developing adolescents.

In order to aid interpretation of the FA findings, longitudinal and radial diffusivities were measured. Previous studies have interpreted FA change in subjects with ASD as a modification in the directional alignment of fibers (Ben Bashat et al., 2007; Catani et al., 2008). Greater FA co-occurring reduced displacement detected in the ASD frontal lobe was interpreted as over-restriction, probably due to reduced synaptic pruning early in development (Ben Bashat et al., 2007). Greater FA associated with reduced radial diffusivity coinciding

with no change of longitudinal diffusivity can result from increased myelin thickness, smaller axonal diameter or extracellular space (Gao et al., 2009). Another study posited that reduced FA in subjects with ASD was due to one of several possibilities, including more obliquely oriented fibers, change in axonal integrity, more not less permeable myelin sheaths, lower axonal density, and abnormal axonal organi-zation (Sundaram et al., 2008). However, these studies excluded measures of longitudinal and radial diffusivities to distinguish among these possibilities. Here, we demonstrated that greater FA values among adolescents with ASD vs. controls in the right superior corona radiata of the cingulate gyrus, right superior longitudinal fasciculus of

Table 3
Regions showing correlation between fractional anisotropy (FA) and age at imaging in 25 subjects with autism spectrum disorder (ASD) vs. in 25 control subjects.

MN Coordinates			Voxel size	White matter tract	Corresponding cortical area	FA mean (SD)		t_{max}	r Correlation between FA and age	
x	y	z				ASD	Control		ASD	Control
10	34	47	12	Right superior longitudinal fasciculus	Superior Frontal Gyrus	0.3034 (0.0348)	0.6641 (0.0435)	**3.98**	−0.343	**0.661**[a]
−9	14	57	13	Left superior longitudinal fasciculus	Superior Frontal Gyrus	0.3135 (0.0397)	0.3183 (0.0638)	**4.15**	−0.044	**0.677**[a]
7	−35	53	33	Right superior longitudinal fasciculus	Paracentral Lobule	0.2958 (0.0490)	0.2927 (0.0617)	**4.19**	−0.464	**0.630**[a]
17	1	49	14	Right superior corona radiata	Cingulate gyrus	0.7263 (0.0703)	0.7180 (0.0660)	**3.66**	−0.061	**0.744**[a]
−18	14	29	30	Corpus callosum	Frontal Lobe	0.5181 (0.0471)	0.5186 (0.0658)	**4.56**	0.267	**0.767**[a]
32	40	−3	11	Right inferior occipitofrontal fasciculus	Frontal Lobe	0.5019 (0.0400)	0.5078 (0.0631)	**3.69**	−0.277	**0.741**[a]

Abbreviation: MNI, Montreal Neurologic Institute.

[a] Boldfaced FA indexes stand for clusters with $t \geq 3.0$ ($P \leq 0.001$ uncorrected) as well as ≥ 10 voxels in voxel-wise correlation analysis between FA and age at imaging. *Bonferroni* corrections were performed (**uncorrected $P \leq 0.004$) in the consideration of multiple tests.
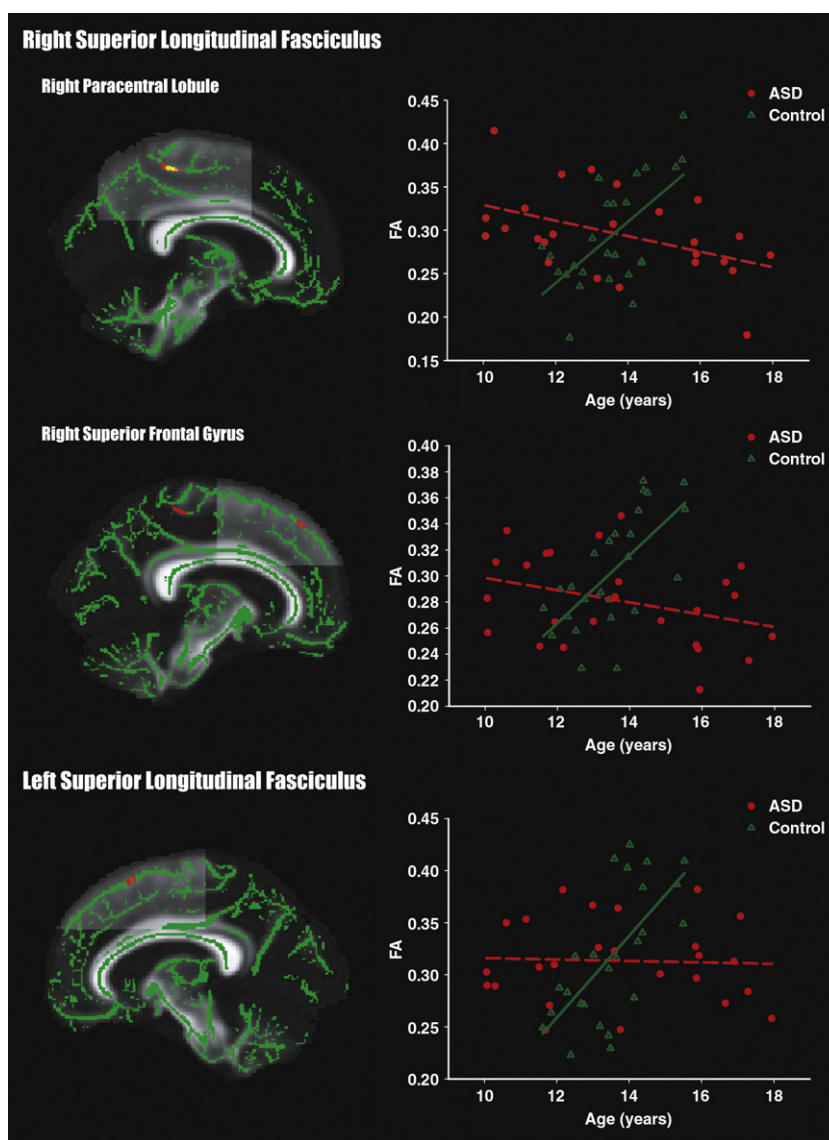
Fig. 3. Correlations between mean fractional anisotropy and age in the ASD and control groups.

insula, middle frontal gyrus, and postcentral gyrus, superior temporal gyrus, and right thalamic radiation were associated with reduced radial diffusivity, consistent with fewer obliquely oriented fibers. Besides, the significant cluster centrally in the tract of the right middle cerebellar peduncle was associated with greater longitudinal diffusivity, consistently with more longitudinally aligned fibers (Versace et al., 2008). Conversely, the association between greater radial diffusivity and reduced FA in participants with ASD vs. controls in the right inferior cerebellar peduncle probably reflected more obliquely oriented fibers, although it also could reflect local inflammatory reaction in subjects with ASD.

A number of studies have indicated that frontal lobe abnormality must play a critical role in high-order social, emotional, and communicational dysfunction in ASD (Courchesne and Pierce, 2005b; Geschwind and Levitt, 2007). At the microscopic level, neuroinflammatory reactions involving glial activation, migration defects, excess cerebral neurogenesis, and/or defective apoptosis might generate frontal neural pathology early in development (Vargas et al., 2005). At the macroscopic level, neuroimaging and neurophysiological investigations revealed that frontal lobe is the driving force for early growth pathology (Belmonte et al., 2004; Carper and Courchesne, 2005; Casanova et al., 2002). Frontal lobe abnormalities include disturbed

external WM radiation and excessive gyrification (Hardan et al., 2004; Herbert et al., 2004). Since the initial findings of reduced functional connectivity between frontal cortex and other lower brain system was in 1988 (Horwitz et al., 1988), there has been disagreement as to whether ASD is a disorder of neural underconnectivity (Just et al., 2007; Just et al., 2004), overconnectivity (Casanova, 2004; Murias et al., 2007), or both, in which long-distance connectivity is decreased but local connectivity is increased (Belmonte et al., 2004; Courchesne and Pierce, 2005b; Koshino et al., 2005). Further, functional neuroimaging during performance of the embedded figures task (Ring et al., 1999), face perception task (Critchley et al., 2000), theory of mind tasks (Castelli et al., 2002; Happe et al., 1996), language tasks (Just et al., 2004), and executive function tasks (Just et al., 2007) have revealed abnormally high activation in low-order sensory processing regions coinciding with reduced activation in frontal areas. The structural and functional abnormalities noted in ASD thus suggest that connectivity within frontal lobe is excessive, disorganized, and inadequately selective, whereas connectivity between frontal cortex and other systems is poorly synchronized (Courchesne and Pierce, 2005b; Courchesne et al., 2007).

Our exploratory analyses revealed significant interaction of age by group mainly in the frontal cortex, which may reflect the core deficit

of ASD. Postmortem data has revealed minicolumn maldevelopment as well as the presence of activated glia and neuroinflammatory response in frontal lobe (Casanova et al., 2002; Vargas et al., 2005). MRI investigations revealed that the growth of the frontal lobe is the driving force for abnormal brain volumes in early ASD (Carper and Courchesne, 2005; Carper et al., 2002). Particularly, increases in cerebral WM volume in the frontal cortex contribute significantly to the general overgrowth in young ASD brains (Herbert et al., 2003; Herbert et al., 2004). DTI scans disclosed greater FA and early accelerated abnormal maturation of WM in the frontal lobe (Ben Bashat et al., 2007). Corroborating behavioral abnormalities have been observed in ASD using paradigms designed to test prefrontal functions, including theory of mind (Castelli et al., 2002; Happe et al., 1996), memory (Koshino et al., 2005; Koshino et al., 2008; Luna et al., 2002), attention (Belmonte and Yurgelun-Todd, 2003), embedded figures (Ring et al., 1999), language (Just et al., 2004), executive function (Just et al., 2007), and emotional processing (Wicker et al., 2008). Many functional neuroimaging studies of ASD have reported abnormal functional responding in the frontal lobe (Hadjikhani et al., 2004; Just et al., 2007; Just et al., 2004; Pierce et al., 2004; Ring et al., 1999) though differences in the primary sensory cortices and ventral temporal regions are also reported (Bolte et al., 2008; Coskun et al., 2009; Gervais et al., 2004). Taken together, these neuroanatomical and neurofunctional representations suggest that frontal cortex in ASD might disturb the effective interaction with other brain regions, as indicated by abnormally increased local connectivity coupled with reduced long-distance frontal-posterior reciprocal connectivity (Courchesne and Pierce, 2005b; Courchesne et al., 2007). The present DTI study demonstrates that ASD impairs the age-related gain in the WM integrity of frontal cortex during adolescence.

The age-related change of frontal lobe FA noted here appears in line with that of temporal lobe FA (Lee et al., 2007), but in contrast with internal capsule (Keller et al., 2007). FA of the right superior temporal gyrus showed minimal association with age in ASD but increased with age in controls in the period from childhood to adulthood (Lee et al., 2007). In contrast, a study found that the posterior limb of internal capsule displayed increasing FA in autism through late adolescence to adulthood, but saw decreasing FA over development in healthy controls (Keller et al., 2007). Importantly, however, the use of cross-sectional experimental design in these studies (including ours) may place limitations on the interpretation of the developmental change observed. We thus argue that the age range of enrolled participants might affect the interaction pattern. During late childhood and adolescence, fiber tracts in the human brain undergo gradual maturation as shown by age-related FA increases in mainly frontotemporal and corticospinal pathways (Ashtari et al., 2007; Barnea-Goraly et al., 2005; Paus et al., 1999; Schmithorst et al., 2005). The maturation of fiber tracts is presumed to play a role in cognitive development. Here we demonstrate that the frontal cortex FA, a reliable indicator of WM integrity, has an age-related gain over development in healthy adolescents, which is not present in subjects with ASD.

One limitation of our study is the lack of inclusion of female participants. The inclusion of only male subjects carries the advantages of sample homogeneity, but limits the generalizability of our results to the entire populations diagnosed with ASD. Further, the ranges of IQ of individuals making up the groups were somewhat uneven (ASD: 74 to 134 vs. control: 94 to 130). These differences may be a confounding source of variability in the size of some of the neural structures we hypothesized as differing between groups (Chiang et al., 2009; Schmithorst et al., 2005). The present study prioritized age matching of groups over IQ matching. Statistically, we attempted to control for IQ effect, by treating as a covariant in our between-group analyses of whole-brain FA. In addition, the study was limited by small and uneven sample size within each ASD subgroup (Autism: Asperger's disorder: PDD-NOS = 11:12:2), which fails to shed further

light into whether the subgroups differ FA abnormalities. Technically, the normalization procedure of TBSS could have difficulties to exactly account for regional abnormalities of frontal WM volume in ASD observed by previous study (Herbert et al., 2004). This may not be the most optimal design, however, and further studies that more tightly control the age and IQ ranges of the larger samples are warranted. Further analysis should take into account the disproportionate increase of WM volume in ASD.

To our knowledge, this is the first study to use TBSS to examine the WM skeleton in individuals with ASD. We found that adolescents with ASD have greater FA and reduced radial diffusivity in the frontal lobe, but experience an age-related loss of FA as compared to the matched controls. Our findings significantly contribute to the growing literatures to highlight a key role of frontal cortex disconnectivity in the pathogenesis of ASD and demonstrate the usefulness of TBSS as a tool for examination of WM in subjects with ASD.

Appendix A. Supplementary data

Supplementary data associated with this article can be found, in the online version, at doi:10.1016/j.neuroimage.2010.01.011.

References

Alexander, A.L., Lee, J.E., Lazar, M., Boudos, R., DuBray, M.B., Oakes, T.R., Miller, J.N., Lu, J., Jeong, E.K., McMahon, W.M., Bigler, E.D., Lainhart, J.E., 2007. Diffusion tensor imaging of the corpus callosum in Autism. NeuroImage 34, 61–73.
Amaral, D.G., Schumann, C.M., Nordahl, C.W., 2008. Neuroanatomy of autism. Trends. Neurosci. 31, 137–145.
Anjari, M., Srinivasan, L., Allsop, J.M., Hajnal, J.V., Rutherford, M.A., Edwards, A.D., Counsell, S.J., 2007. Diffusion tensor imaging with tract-based spatial statistics reveals local white matter abnormalities in preterm infants. NeuroImage 35, 1021–1027.
Arfanakis, K., Haughton, V.M., Carew, J.D., Rogers, B.P., Dempsey, R.J., Meyerand, M.E., 2002. Diffusion tensor MR imaging in diffuse axonal injury. AJNR. Am. J. Neuroradiol. 23, 794–802.
Arnone, D., Barrick, T.R., Chengappa, S., Mackay, C.E., Clark, C.A., Abou-Saleh, M.T., 2008. Corpus callosum damage in heavy marijuana use: preliminary evidence from diffusion tensor tractography and tract-based spatial statistics. NeuroImage 41, 1067–1074.
Ashtari, M., Cervellione, K.L., Hasan, K.M., Wu, J., McIlree, C., Kester, H., Ardekani, B.A., Roofeh, D., Szeszko, P.R., Kumra, S., 2007. White matter development during late adolescence in healthy males: a cross-sectional diffusion tensor imaging study. NeuroImage 35, 501–510.
Baratti, C., Barnett, A.S., Pierpaoli, C., 1999. Comparative MR imaging study of brain maturation in kittens with T1, T2, and the trace of the diffusion tensor. Radiology 210, 133–142.
Barnea-Goraly, N., Kwon, H., Menon, V., Eliez, S., Lotspeich, L., Reiss, A.L., 2004. White matter structure in autism: preliminary evidence from diffusion tensor imaging. Biol. Psychiatry 55, 323–326.
Barnea-Goraly, N., Menon, V., Eckert, M., Tamm, L., Bammer, R., Karchemskiy, A., Dant, C.C., Reiss, A.L., 2005. White matter development during childhood and adolescence: a cross-sectional diffusion tensor imaging study. Cereb. Cortex 15, 1848–1854.
Barnea-Goraly, N., Chang, K.D., Karchemskiy, A., Howe, M.E., Reiss, A.L., 2009. Limbic and corpus callosum aberrations in adolescents with bipolar disorder: a tract-based spatial statistics analysis. Biol. Psychiatry 66 (3), 238–244.
Baron-Cohen, S., Belmonte, M.K., 2005. Autism: a window onto the development of the social and the analytic brain. Annu. Rev. Neurosci. 28, 109–126.
Beaulieu, C., 2002. The basis of anisotropic water diffusion in the nervous system- a technical review. NMR Biomed. 15, 435–455.
Belmonte, M.K., Yurgelun-Todd, D.A., 2003. Functional anatomy of impaired selective attention and compensatory processing in autism. Brain Res. Cogn. Brain Res. 17, 651–664.
Belmonte, M.K., Allen, G., Beckel-Mitchener, A., Boulanger, L.M., Carper, R.A., Webb, S.J., 2004. Autism and abnormal development of brain connectivity. J. Neurosci. 24, 9228–9231.

Ben Bashat, D., Kronfeld-Duenias, V., Zachor, D.A., Ekstein, P.M., Hendler, T., Tarrasch, R., Even, A., Levy, Y., Ben Sira, L., 2007. Accelerated maturation of white matter in young children with autism: a high b value DWI study. NeuroImage 37, 40–47.

Bodini, B., Khaleeli, Z., Cercignani, M., Miller, D.H., Thompson, A.J., Ciccarelli, O., 2009. Exploring the relationship between white matter and gray matter damage in early primary progressive multiple sclerosis: an in vivo study with TBSS and VBM. Hum. Brain Mapp. 30 (9), 2852–2861.

Bolte, S., Hubl, D., Dierks, T., Holtmann, M., Poustka, F., 2008. An fMRI-study of locally oriented perception in autism: altered early visual processing of the block design test. J. Neural Transm. 115, 545–552.

Budde, M.D., Kim, J.H., Liang, H.F., Russell, J.H., Cross, A.H., Song, S.K., 2008. Axonal injury detected by in vivo diffusion tensor imaging correlates with neurological disability in a mouse model of multiple sclerosis. NMR Biomed. 21, 589–597.

Cader, S., Johansen-Berg, H., Wylezinska, M., Palace, J., Behrens, T.E., Smith, S., Matthews, P.M., 2007. Discordant white matter N-acetylasparate and diffusion MRI measures suggest that chronic metabolic dysfunction contributes to axonal pathology in multiple sclerosis. NeuroImage 36, 19–27.

Carper, R.A., Courchesne, E., 2005. Localized enlargement of the frontal cortex in early autism. Biol. Psychiatry 57, 126–133.

Carper, R.A., Moses, P., Tigue, Z.D., Courchesne, E., 2002. Cerebral lobes in autism: early hyperplasia and abnormal age effects. NeuroImage 16, 1038–1051.

Casanova, M.F., 2004. White matter volume increase and minicolumns in autism. Ann. Neurol. 56, 453 author reply 454.

Casanova, M.F., Buxhoeveden, D.P., Switala, A.E., Roy, E., 2002. Minicolumnar pathology in autism. Neurology 58, 428–432.

Castelli, F., Frith, C., Happe, F., Frith, U., 2002. Autism, Asperger syndrome and brain mechanisms for the attribution of mental states to animated shapes. Brain 125, 1839–1849.

Catani, M., Jones, D.K., Daly, E., Embiricos, N., Deeley, Q., Pugliese, L., Curran, S., Robertson, D., Murphy, D.G., 2008. Altered cerebellar feedback projections in Asperger syndrome. NeuroImage 41, 1184–1191.

Chiang, M.C., Barysheva, M., Shattuck, D.W., Lee, A.D., Madsen, S.K., Avedissian, C., Klunder, A.D., Toga, A.W., McMahon, K.L., de Zubicaray, G.I., Wright, M.J., Srivastava, A., Balov, N., Thompson, P.M., 2009. Genetics of brain fiber architecture and intellectual performance. J. Neurosci. 29, 2212–2224.

Choi, J., Jeong, B., Rohan, M.L., Polcari, A.M., Teicher, M.H., 2009. Preliminary evidence for white matter tract abnormalities in young adults exposed to parental verbal abuse. Biol. Psychiatry 65, 227–234.

Concha, L., Beaulieu, C., Gross, D.W., 2005. Bilateral limbic diffusion abnormalities in unilateral temporal lobe epilepsy. Ann. Neurol. 57, 188–196.

Conturo, T.E., Williams, D.L., Smith, C.D., Gultepe, E., Akbudak, E., Minshew, N.J., 2008. Neuronal fiber pathway abnormalities in autism: an initial MRI diffusion tensor tracking study of hippocampo-fusiform and amygdalo-fusiform pathways. J. Int. Neuropsychol. Soc. 14, 933–946.

Coskun, M.A., Varghese, L., Reddoch, S., Castillo, E.M., Pearson, D.A., Loveland, K.A., Papanicolaou, A.C., Sheth, B.R., 2009. How somatic cortical maps differ in autistic and typical brains. NeuroReport 20, 175–179.

Courchesne, E., Carper, R., Akshoomoff, N., 2003. Evidence of brain overgrowth in the first year of life in autism. JAMA 290, 337–344.

Courchesne, E., Pierce, K., 2005a. Brain overgrowth in autism during a critical time in development: implications for frontal pyramidal neuron and interneuron development and connectivity. Int. J. Dev. Neurosci. 23, 153–170.

Courchesne, E., Pierce, K., 2005b. Why the frontal cortex in autism might be talking only to itself: local over-connectivity but long-distance disconnection. Curr. Opin. Neurobiol. 15, 225–230.

Courchesne, E., Pierce, K., Schumann, C.M., Redcay, E., Buckwalter, J.A., Kennedy, D.P., Morgan, J., 2007. Mapping early brain development in autism. Neuron 56, 399–413.

Critchley, H.D., Daly, E.M., Bullmore, E.T., Williams, S.C., Van Amelsvoort, T., Robertson, D.M., Rowe, A., Phillips, M., McAlonan, G., Howlin, P., Murphy, D.G., 2000. The functional neuroanatomy of social behaviour: changes in cerebral blood flow when people with autistic disorder process facial expressions. Brain 123 (Pt. 11), 2203–2212.

Dawson, G., Munson, J., Webb, S.J., Nalty, T., Abbott, R., Toth, K., 2007. Rate of head growth decelerates and symptoms worsen in the second year of life in autism. Biol. Psychiatry 61, 458–464.

Dementieva, Y.A., Vance, D.D., Donnelly, S.L., Elston, L.A., Wolpert, C.M., Ravan, S.A., DeLong, G.R., Abramson, R.K., Wright, H.H., Cuccaro, M.L., 2005. Accelerated head growth in early development of individuals with autism. Pediatr. Neurol. 32, 102–108.

Dineen, R.A., Vilisaar, J., Hlinka, J., Bradshaw, C.M., Morgan, P.S., Constantinescu, C.S., Auer, D.P., 2009. Disconnection as a mechanism for cognitive dysfunction in multiple sclerosis. Brain 132, 239–249.

Douaud, G., Smith, S., Jenkinson, M., Behrens, T., Johansen-Berg, H., Vickers, J., James, S., Voets, N., Watkins, K., Matthews, P.M., James, A., 2007. Anatomically related grey and white matter abnormalities in adolescent-onset schizophrenia. Brain 130, 2375–2386.

Engelbrecht, V., Scherer, A., Rassek, M., Witsack, H.J., Modder, U., 2002. Diffusion-weighted MR imaging in the brain in children: findings in the normal brain and in the brain with white matter diseases. Radiology 222, 410–418.

Gao, W., Lin, W., Chen, Y., Gerig, G., Smith, J.K., Jewells, V., Gilmore, J.H., 2009. Temporal and spatial development of axonal maturation and myelination of white matter in the developing brain. AJNR. Am. J. Neuroradiol. 30, 290–296.

Gervais, H., Belin, P., Boddaert, N., Leboyer, M., Coez, A., Sfaello, I., Barthelemy, C., Brunelle, F., Samson, Y., Zilbovicius, M., 2004. Abnormal cortical voice processing in autism. Nat. Neurosci. 7, 801–802.

Geschwind, D.H., Levitt, P., 2007. Autism spectrum disorders: developmental disconnection syndromes. Curr. Opin. Neurobiol. 17, 103–111.

Giorgio, A., Watkins, K.E., Douaud, G., James, A.C., James, S., De Stefano, N., Matthews, P.M., Smith, S.M., Johansen-Berg, H., 2008. Changes in white matter microstructure during adolescence. NeuroImage 39, 52–61.

Hadjikhani, N., Chabris, C.F., Joseph, R.M., Clark, J., McGrath, L., Aharon, I., Feczko, E., Tager-Flusberg, H., Harris, G., 2004. Early visual cortex organization in autism: an fMRI study. NeuroReport 15, 267–270.

Happe, F., Ehlers, S., Fletcher, P., Frith, U., Johansson, M., Gillberg, C., Dolan, R., Frackowiak, R., Frith, C., 1996. 'Theory of mind' in the brain. Evidence from a PET scan study of Asperger syndrome. NeuroReport 8, 197–201.

Hardan, A.Y., Jou, R.J., Keshavan, M.S., Varma, R., Minshew, N.J., 2004. Increased frontal cortical folding in autism: a preliminary MRI study. Psychiatry Res. 131, 263–268.

Hasan, K.M., Narayana, P.A., 2006. Retrospective measurement of the diffusion tensor eigenvalues from diffusion anisotropy and mean diffusivity in DTI. Magn. Reson. Med. 56, 130–137.

Hazlett, H.C., Poe, M.D., Gerig, G., Smith, R.G., Piven, J., 2006. Cortical gray and white brain tissue volume in adolescents and adults with autism. Biol. Psychiatry 59, 1–6.

Herbert, M.R., Ziegler, D.A., Deutsch, C.K., O'Brien, L.M., Lange, N., Bakardjiev, A., Hodgson, J., Adrien, K.T., Steele, S., Makris, N., Kennedy, D., Harris, G.J., Caviness Jr, V.S., 2003. Dissociations of cerebral cortex, subcortical and cerebral white matter volumes in autistic boys. Brain 126, 1182–1192.

Herbert, M.R., Ziegler, D.A., Makris, N., Filipek, P.A., Kemper, T.L., Normandin, J.J., Sanders, H.A., Kennedy, D.N., Caviness Jr, V.S., 2004. Localization of white matter volume increase in autism and developmental language disorder. Ann. Neurol. 55, 530–540.

Hoeft, F., Barnea-Goraly, N., Haas, B.W., Golarai, G., Ng, D., Mills, D., Korenberg, J., Bellugi, U., Galaburda, A., Reiss, A.L., 2007. More is not always better: increased fractional anisotropy of superior longitudinal fasciculus associated with poor visuospatial abilities in Williams syndrome. J. Neurosci. 27, 11960–11965.

Horwitz, B., Rumsey, J.M., Grady, C.L., Rapoport, S.I., 1988. The cerebral metabolic landscape in autism. Intercorrelations of regional glucose utilization. Arch. Neurol. 45, 749–755.

Huppi, P.S., Maier, S.E., Peled, S., Zientara, G.P., Barnes, P.D., Jolesz, F.A., Volpe, J.J., 1998. Microstructural development of human newborn cerebral white matter assessed in vivo by diffusion tensor magnetic resonance imaging. Pediatr. Res. 44, 584–590.

Jones, D.K., Symms, M.R., Cercignani, M., Howard, R.J., 2005. The effect of filter size on VBM analyses of DT-MRI data. NeuroImage 26, 546–554.

Just, M.A., Cherkassky, V.L., Keller, T.A., Minshew, N.J., 2004. Cortical activation and synchronization during sentence comprehension in high-functioning autism: evidence of underconnectivity. Brain 127, 1811–1821.

Just, M.A., Cherkassky, V.L., Keller, T.A., Kana, R.K., Minshew, N.J., 2007. Functional and anatomical cortical underconnectivity in autism: evidence from an FMRI study of an executive function task and corpus callosum morphometry. Cereb. Cortex 17, 951–961.

Karlsgodt, K.H., van Erp, T.G., Poldrack, R.A., Bearden, C.E., Nuechterlein, K.H., Cannon, T.D., 2008. Diffusion tensor imaging of the superior longitudinal fasciculus and working memory in recent-onset schizophrenia. Biol. Psychiatry 63, 512–518.

Keller, T.A., Kana, R.K., Just, M.A., 2007. A developmental study of the structural integrity of white matter in autism. NeuroReport 18, 23–27.

Koshino, H., Carpenter, P.A., Minshew, N.J., Cherkassky, V.L., Keller, T.A., Just, M.A., 2005. Functional connectivity in an fMRI working memory task in high-functioning autism. NeuroImage 24, 810–821.

Koshino, H., Kana, R.K., Keller, T.A., Cherkassky, V.L., Minshew, N.J., Just, M.A., 2008. fMRI investigation of working memory for faces in autism: visual coding and underconnectivity with frontal areas. Cereb. Cortex 18, 289–300.

Le Bihan, D., 1995. Molecular diffusion, tissue microdynamics and microstructure. NMR. Biomed. 8, 375–386.

Lee, J.E., Bigler, E.D., Alexander, A.L., Lazar, M., DuBray, M.B., Chung, M.K., Johnson, M., Morgan, J., Miller, J.N., McMahon, W.M., Lu, J., Jeong, E.K., Lainhart, J.E., 2007. Diffusion tensor imaging of white matter in the superior temporal gyrus and temporal stem in autism. Neurosci. Lett. 424, 127–132.

Li, L., Coles, C.D., Lynch, M.E., Hu, X., 2009. Voxelwise and skeleton-based region of interest analysis of fetal alcohol syndrome and fetal alcohol spectrum disorders in young adults. Hum. Brain Mapp. 30 (10), 3265–3274.

Lotspeich, L.J., Kwon, H., Schumann, C.M., Fryer, S.L., Goodlin-Jones, B.L., Buonocore, M.H., Lammers, C.R., Amaral, D.G., Reiss, A.L., 2004. Investigation of neuroanatomical differences between autism and Asperger syndrome. Arch. Gen. Psychiatry 61, 291–298.

Luna, B., Minshew, N.J., Garver, K.E., Lazar, N.A., Thulborn, K.R., Eddy, W.F., Sweeney, J.A., 2002. Neocortical system abnormalities in autism: an fMRI study of spatial working memory. Neurology 59, 834–840.

Minshew, N.J., Goldstein, G., Siegel, D.J., 1997. Neuropsychologic functioning in autism: profile of a complex information processing disorder. J. Int. Neuropsychol. Soc. 3, 303–316.

Mukherjee, P., McKinstry, R.C., 2006. Diffusion tensor imaging and tractography of human brain development. Neuroimaging Clin. N. Am. 16, 19–43 vii.

Mukherjee, P., Miller, J.H., Shimony, J.S., Philip, J.V., Nehra, D., Snyder, A.Z., Conturo, T.E., Neil, J.J., McKinstry, R.C., 2002. Diffusion-tensor MR imaging of gray and white matter development during normal human brain maturation. AJNR Am. J. Neuroradiol. 23, 1445–1456.

Murias, M., Webb, S.J., Greenson, J., Dawson, G., 2007. Resting state cortical connectivity reflected in EEG coherence in individuals with autism. Biol. Psychiatry 62, 270–273.

Neil, J.J., Shiran, S.I., McKinstry, R.C., Schefft, G.L., Snyder, A.Z., Almli, C.R., Akbudak, E.,

Aronovitz, J.A., Miller, J.P., Lee, B.C., Conturo, T.E., 1998. Normal brain in human newborns: apparent diffusion coefficient and diffusion anisotropy measured by using diffusion tensor MR imaging. Radiology 209, 57–66.

Neil, J., Miller, J., Mukherjee, P., Huppi, P.S., 2002. Diffusion tensor imaging of normal and injured developing human brain—a technical review. NMR Biomed. 15, 543–552.

Nunnemann, S., Wohlschlager, A.M., Ilg, R., Gaser, C., Etgen, T., Conrad, B., Zimmer, C., Muhlau, M., 2009. Accelerated aging of the putamen in men but not in women. Neurobiol. Aging 30, 147–151.

Palmen, S.J., Hulshoff Pol, H.E., Kemner, C., Schnack, H.G., Durston, S., Lahuis, B.E., Kahn, R.S., Van Engeland, H., 2005. Increased gray-matter volume in medication-naive high-functioning children with autism spectrum disorder. Psychol. Med. 35, 561–570.

Paus, T., Zijdenbos, A., Worsley, K., Collins, D.L., Blumenthal, J., Giedd, J.N., Rapoport, J.L., Evans, A.C., 1999. Structural maturation of neural pathways in children and adolescents: in vivo study. Science 283, 1908–1911.

Pierce, K., Haist, F., Sedaghat, F., Courchesne, E., 2004. The brain response to personally familiar faces in autism: findings of fusiform activity and beyond. Brain 127, 2703–2716.

Ring, H.A., Baron-Cohen, S., Wheelwright, S., Williams, S.C., Brammer, M., Andrew, C., Bullmore, E.T., 1999. Cerebral correlates of preserved cognitive skills in autism: a functional MRI study of embedded figures task performance. Brain 122 (Pt. 7), 1305–1315.

Roosendaal, S.D., Geurts, J.J., Vrenken, H., Hulst, H.E., Cover, K.S., Castelijns, J.A., Pouwels, P.J., Barkhof, F., 2009. Regional DTI differences in multiple sclerosis patients. NeuroImage 44, 1397–1403.

Rueckert, D., Sonoda, L.I., Hayes, C., Hill, D.L., Leach, M.O., Hawkes, D.J., 1999. Nonrigid registration using free-form deformations: application to breast MR images. IEEE Trans. Med. Imaging 18, 712–721.

Sage, C.A., Van Hecke, W., Peeters, R., Sijbers, J., Robberecht, W., Parizel, P., Marchal, G., Leemans, A., Sunaert, S., 2009. Quantitative diffusion tensor imaging in amyotrophic lateral sclerosis: Revisited. Hum. Brain Mapp. 30 (11), 3657–3675.

Schmithorst, V.J., Wilke, M., Dardzinski, B.J., Holland, S.K., 2005. Cognitive functions correlate with white matter architecture in a normal pediatric population: a diffusion tensor MRI study. Hum. Brain Mapp. 26, 139–147.

Schoene-Bake, J.C., Faber, J., Trautner, P., Kaaden, S., Tittgemeyer, M., Elger, C.E., Weber, B., 2009. Widespread affections of large fiber tracts in postoperative temporal lobe epilepsy. NeuroImage 46, 569–576.

Schumann, C.M., Amaral, D.G., 2006. Stereological analysis of amygdala neuron number in autism. J. Neurosci. 26, 7674–7679.

Schumann, C.M., Hamstra, J., Goodlin-Jones, B.L., Lotspeich, L.J., Kwon, H., Buonocore, M.H., Lammers, C.R., Reiss, A.L., Amaral, D.G., 2004. The amygdala is enlarged in children but not adolescents with autism; the hippocampus is enlarged at all ages. J. Neurosci. 24, 6392–6401.

Schwartz, E.D., Hackney, D.B., 2003. Diffusion-weighted MRI and the evaluation of spinal cord axonal integrity following injury and treatment. Exp. Neurol. 184, 570–589.

Silk, T.J., Vance, A., Rinehart, N., Bradshaw, J.L., Cunnington, R., 2009. White-matter abnormalities in attention deficit hyperactivity disorder: a diffusion tensor imaging study. Hum. Brain Mapp. 30 (9), 2757–2765.

Smith, S.M., 2002. Fast robust automated brain extraction. Hum. Brain. Mapp. 17, 143–155.

Smith, S.M., Jenkinson, M., Woolrich, M.W., Beckmann, C.F., Behrens, T.E., Johansen-Berg, H., Bannister, P.R., De Luca, M., Drobnjak, I., Flitney, D.E., Niazy, R.K., Saunders, J., Vickers, J., Zhang, Y., De Stefano, N., Brady, J.M., Matthews, P.M., 2004. Advances in functional and structural MR image analysis and implementation as FSL. Neuroimage 23 (Suppl. 1), S208–S219.

Smith, S.M., Jenkinson, M., Johansen-Berg, H., Rueckert, D., Nichols, T.E., Mackay, C.E., Watkins, K.E., Ciccarelli, O., Cader, M.Z., Matthews, P.M., Behrens, T.E., 2006. Tract-based spatial statistics: voxelwise analysis of multi-subject diffusion data. NeuroImage 31, 1487–1505.

Smith, S.M., Johansen-Berg, H., Jenkinson, M., Rueckert, D., Nichols, T.E., Miller, K.L., Robson, M.D., Jones, D.K., Klein, J.C., Bartsch, A.J., Behrens, T.E., 2007. Acquisition and voxelwise analysis of multi-subject diffusion data with tract-based spatial statistics. Nat. Protoc. 2, 499–503.

Smith, C.D., Chebrolu, H., Andersen, A.H., Powell, D.A., Lovell, M.A., Xiong, S., Gold, B.T., in press. White matter diffusion alterations in normal women at risk of Alzheimer's disease. Neurobiol. Aging in press. doi:10.1016/j.neurobiolaging.2008.08.006.

Song, S.K., Sun, S.W., Ramsbottom, M.J., Chang, C., Russell, J., Cross, A.H., 2002. Dysmyelination revealed through MRI as increased radial (but unchanged axial) diffusion of water. NeuroImage 17, 1429–1436.

Song, S.K., Sun, S.W., Ju, W.K., Lin, S.J., Cross, A.H., Neufeld, A.H., 2003. Diffusion tensor imaging detects and differentiates axon and myelin degeneration in mouse optic nerve after retinal ischemia. NeuroImage 20, 1714–1722.

Sparks, B.F., Friedman, S.D., Shaw, D.W., Aylward, E.H., Echelard, D., Artru, A.A., Maravilla, K.R., Giedd, J.N., Munson, J., Dawson, G., Dager, S.R., 2002. Brain structural abnormalities in young children with autism spectrum disorder. Neurology 59, 184–192.

Stricker, N.H., Schweinsburg, B.C., Delano-Wood, L., Wierenga, C.E., Bangen, K.J., Haaland, K.Y., Frank, L.R., Salmon, D.P., Bondi, M.W., 2009. Decreased white matter integrity in late-myelinating fiber pathways in Alzheimer's disease supports retrogenesis. NeuroImage 45, 10–16.

Sundaram, S.K., Kumar, A., Makki, M.I., Behen, M.E., Chugani, H.T., Chugani, D.C., 2008. Diffusion tensor imaging of frontal lobe in autism spectrum disorder. Cereb. Cortex 18, 2659–2665.

Thakkar, K.N., Polli, F.E., Joseph, R.M., Tuch, D.S., Hadjikhani, N., Barton, J.J., Manoach, D.S., 2008. Response monitoring, repetitive behaviour and anterior cingulate abnormalities in autism spectrum disorders (ASD). Brain 131, 2464–2478.

Thomalla, G., Glauche, V., Koch, M.A., Beaulieu, C., Weiller, C., Rother, J., 2004. Diffusion tensor imaging detects early Wallerian degeneration of the pyramidal tract after ischemic stroke. NeuroImage 22, 1767–1774.

Tuch, D.S., Salat, D.H., Wisco, J.J., Zaleta, A.K., Hevelone, N.D., Rosas, H.D., 2005. Choice reaction time performance correlates with diffusion anisotropy in white matter pathways supporting visuospatial attention. Proc. Natl. Acad. Sci. U. S. A. 102, 12212–12217.

Van Naarden Braun, K., Pettygrove, S., Daniels, J., Miller, L., Nicholas, J., Baio, J., Schieve, L., Kirby, R.S., Washington, A., Brocksen, S., Rahbar, H., Rice, C., 2007. Evaluation of a methodology for a collaborative multiple source surveillance network for autism spectrum disorders–Autism and Developmental Disabilities Monitoring Network, 14 sites, United States, 2002. MMWR Surveill. Summ. 56, 29–40.

Vargas, D.L., Nascimbene, C., Krishnan, C., Zimmerman, A.W., Pardo, C.A., 2005. Neuroglial activation and neuroinflammation in the brain of patients with autism. Ann. Neurol. 57, 67–81.

Versace, A., Almeida, J.R., Hassel, S., Walsh, N.D., Novelli, M., Klein, C.R., Kupfer, D.J., Phillips, M.L., 2008. Elevated left and reduced right orbitomedial prefrontal fractional anisotropy in adults with bipolar disorder revealed by tract-based spatial statistics. Arch. Gen. Psychiatry 65, 1041–1052.

Wechsler, D., 1991. Wechsler Intelligence Scale for Children3rd ed. The Psychological Corporation, San Antonia, TX.

WHO, 1994. International classification of diseases, 10 ed. World Health Organization, Geneva.

Wicker, B., Fonlupt, P., Hubert, B., Tardif, C., Gepner, B., Deruelle, C., 2008. Abnormal cerebral effective connectivity during explicit emotional processing in adults with autism spectrum disorder. Soc. Cogn. Affect. Neurosci. 3, 135–143.